**EUROPEAN ORGANIZATION FOR NUCLEAR RESEARCH**
**European Laboratory for Particle Physics**


**Internal Note/**
ALICE reference number

ALICE-INT-2011-XXX version 1.0

Date of last change: 30.05.2011

# Comparison of hit-track matching efficiency with single-sided and double-sided layers

**Authors:**

J. Baudot, S. Senyukov

*IPHC/ IN2P3-CNRS, Université de Strasbourg*

## Abstract

The technology of CMOS pixel sensors, or MAPS, is offering a new optimization between pixel granularity, readout speed, power dissipation and material budget compared to technologies employed so far in high energy physics experiments. Consequently, new approaches are emerging to integrate such detectors. One of them consists in building double-sided detection layers which provide two real-2D points whereas standard single-sided layers provides only one.
In this note, we explore the potential benefits of such double-sided layers for the specific problem of associating hits with tracks. Indeed, large experiments usually dedicate separate sub-detectors for the *tracking* and the *vertexing*. In such a case, reconstructed tracks need to be matched with their corresponding hits in the, usually discrete, layers of the vertex detector. The efficiency of this matching step for a given layer depends on the hit density, the uncertainty on the track parameters at this layer -wich embeds the geometry and spatial resolution of the previous layers- and, of course, on the spatial accuracy of the layer itself.

# 1 Introduction

An essential step of any tracking algorithm consists in associating hits together to form a track. In this note, we consider the specific case of the association of hits measured in a vertex detector, with tracks that have been already reconstructed by a tracker surrounding the vertex detector. This is the typical case of experiments like STAR, ALICE or ILD where tracking proceeds in two steps. Firstly, a time projection chamber (TPC) allows to individualize tracks. Then those tracks are extrapolated toward the primary collision vertex with the help of several inner layers. The extrapolation goes from one layer to the other, starting at the largest radius. The hit associated at each layer is used to update the track parameters. The track extrapolation accuracy toward the next layer increases with decreasing radius which helps to fight against the increasing hit density.

For the purpose of optimizing the design of new detectors, it is extremely useful to predict the efficiency of the hit-track association for a given detector configuration. We define the matching efficiency at a given layer as the probability to associate the track reconstructed for a particle trajectory to the hit generated by this same particle in the layer.
One source of inefficiency is due to the detection efficiency $\epsilon_{det}$ of the layer not being 100 %. If considering a double-sided layer the probability to get at least one measurement point is $(1 - (1 - \epsilon_{det})^2)$ to be compared to $\epsilon_{det}$ for a single-sided layer. The gain obtained with the double-sided layer quantifies to $\epsilon_{det} \times (1 - \epsilon_{det})$ which is about 2% and 5% for $\epsilon_{det} = 98\%$ and 95% respectively. We shall not discuss further this point.
The other part of the inefficiency for matching a track with the corresponding hit stems from the presence on the layer of other hits than the one looked for. One easily understands that, if the hit is searched for in a given area, the probability depends on the hit density, the surface of the search area, the accuracy of the hit location and the criteria to select a hit. The exact expression for single-sided layers was derived analytically in [1] in the framework of the STAR Heavy Flavor Tracker design [2] study.

This work generalizes the computation of the matching efficiency for a double-sided layer. Such a layer provides two independent measurements with a radii difference of about 2 mm [3]. This set of two points allows to estimate the direction of the propagating track and not only its position at the layer radius. It is expected that the additional constraint improves the matching efficiency.
However, the number of so-called mini-vectors built from the combination of any of the hits present on the two sides of the layer increases like the square of the hit density. This fact tends to decrease the probability to match the correct hit. In other words, the single-sided case corresponds to a two dimensional problem

whereas the double-sided case is a problem in four dimensions. Our goal is to investigate in which domain of the parameter space the double-sided approach is beneficial or detrimental.

The next section establishes the probability expression in the general case, then comparative results for the single-sided and double-sided layer cases are discussed in the last section.

# 2 General formula for the matching efficiency

## 2.1 Matching procedure

Sections 2.1 & 2.2 consider a n-dimension space. This is a more complex case than what we considered, where n = 1 (section 2.3).

Before deriving a formula for the efficiency, we shall describe the matching procedure. It is based on the $\chi^2$ approach as introduced in [1].
We define the typical collider geometry where the $z$ axis is parallel to the beam axis and the $R\phi$ plane is perpendicular to it. We localize a point in the local planar geometry of a given layer at a radius $r$ with the coordinates $(x, z)$ where the $x$ axis is perpendicular to the beam and the radius.

A track, with a given direction is extrapolated inward on a layer at a known radius $(r)$ with a pointing accuracy $\sigma_{ext,R\phi}(r)$ in the transverse plane and $\sigma_{ext,z}(r)$ along the beam axis. The layer itself features an intrinsic spatial resolution in both directions respectively $\sigma_{int,R\phi}(r)$ and $\sigma_{int,z}(r)$. The following $\chi^2$ provides a quantitative estimation of the matching quality between the track extrapolation crossing the layer at $x_t, z_t$ and a hit located at position $x_p, z_p$ on this layer:

$$\chi^2(x_p, z_p) = \frac{(x_t - x_p)^2}{\sigma^2_{\text{eff,R}\phi}} + \frac{(z_t - z_p)^2}{\sigma^2_{\text{eff,z}}}. \tag{1}$$

The standard deviations used in the previous equation are defined as the quadratic sum of the extrapolated and intrinsic spatial resolution in both directions: $\sigma^2_{\text{eff}} = \sigma^2_{ext} + \sigma^2_{int}$. Usually $\sigma_{ext} \gg \sigma_{int}$, so we denote the overall $\sigma_{\text{eff}}$ as an effective spatial resolution in the following. The hit with the lowest $\chi^2$ is chosen for the association.

When matching simultaneously two layers at different radii $r_1$ and $r_2$, the $\chi^2$ properties authorize a simple sum of both $\chi^2$ corresponding to a couple of points $((x_{1,p}, z_{1,p}), (x_{2,p}, z_{2,p}))$ associated with effective uncertainties for each layer, respectively $((\sigma_{\text{eff1,R}\phi}, \sigma_{\text{eff1,z}}), (\sigma_{\text{eff2,R}\phi}, \sigma_{\text{eff2,z}}))$:

$$\chi^2(x_{1,p}, z_{1,p}, x_{2,p}, z_{2,p}) = \frac{(x_{1,t} - x_{1,p})^2}{\sigma^2_{\text{eff1,R}\phi}} + \frac{(z_{1,t} - z_{1,p})^2}{\sigma^2_{\text{eff1,z}}} + \frac{(x_{2,t} - x_{2,p})^2}{\sigma^2_{\text{eff2,R}\phi}} + \frac{(z_{2,t} - z_{2,p})^2}{\sigma^2_{\text{eff2,z}}}. \tag{2}$$

The mini-vector, which can be built out of the two points, does not appear explicitly in the previous equation. Indeed, no angle is computed that can be compared to the track parameters. However, equation 2 implicitly contains this comparison since the track projections in both layers $((x_{1,t}, z_{1,t}), (x_{2,t}, z_{2,t}))$ and their uncertainties are taken into account simultaneously. This approach also copes naturally with non-straight tracks.

We observe that the $\chi^2$ dimension, or number of parameters, increases from 2 with a single-sided layer to 4 with a double-sided layer. Generalizing, trying to match $n$ 2D measurements simultaneously would lead to a $2n$ dimensional problems. Mathematically the matrix formalism is best suited to deal with any number of dimensions. So we define the following $2n$-vector and $2n \times 2n$-matrix:

$$\vec{X} = [x_{1,t} - x_{1,p}, z_{1,t} - z_{1,p}, ..., x_{n,t} - x_{n,p}, z_{n,t} - z_{n,p}], \tag{3}$$

$$\Sigma^{-1} = \begin{pmatrix} \frac{1}{\sigma^2_{\mathrm{eff}1,\mathrm{R}\phi}} & 0 & ... & 0 & 0 \\ 0 & \frac{1}{\sigma^2_{\mathrm{eff}1,\mathrm{z}}} & ... & 0 & 0 \\ ... & ... & ... & ... & ... \\ 0 & 0 & ... & \frac{1}{\sigma^2_{\mathrm{eff}n,\mathrm{R}\phi}} & 0 \\ 0 & 0 & ... & 0 & \frac{1}{\sigma^2_{\mathrm{eff}n,\mathrm{z}}} \end{pmatrix}. \tag{4}$$

The vector $\vec{X}$ contains the two coordinates of each 2D vector joining a hit and the track on a given side. The weight matrix $\Sigma^{-1}$ is the usual inverse of the covariance matrix which allows to obtain the general $\chi^2$ expression:

$$\chi^2(\vec{X}) = \vec{X}^T \Sigma^{-1} \vec{X}. \tag{5}$$

The set of $n$ hits related to the track is searched as the one with the minimal $\chi^2$ of all the sets of $n$hits located in a $2n$-volume (noted $V_{2n}$ in the following) centered on the track extrapolation and extended in each dimension by $\pm f \times \sigma_{\mathrm{eff}}$ where $f$ is usually above 3. Indeed, lower values of $f$ would limit the matching efficiency due to an insufficient search area.

## 2.2 Computing the matching efficiency

Computing the matching efficiency is equivalent to the estimation of the probability $P_{n,match}$ that the real set of $n$ hits generated by the particle is present in the searched $2n$-volume $V_{2n}$ and has the minimal $\chi^2$ of all the sets of $n$ hits in this volume. The latter writes as an $2n$-dimensional integral over the volume $V_{2n}$

$$P_{n,match} = \int_{V_{2n}} P_{nh}(\vec{X}) \times \frac{\mathrm{d}P_h(\vec{X})}{\mathrm{d}\vec{X}} \, \mathrm{d}^{2n}\vec{X}, \tag{6}$$

where

- $\frac{\mathrm{d}P_h(\vec{X})}{\mathrm{d}\vec{X}}\,\mathrm{d}^{2n}\vec{X}$ is the probability that the true set of hits generated by the particle is located in an elementary volume $\mathrm{d}\vec{X}$ around the position $\vec{X}$,
- $P_{nh}(\vec{X})$ is the probability that no other set of $n$ hits has a $\chi^2$ lower than the true hit.

The probability density that the correct set of $n$ hits lies at the position $\vec{X}$ is simply a $2n$-dimensional normal distribution:

$$\frac{\mathrm{d}P_h(\vec{X})}{\mathrm{d}\vec{X}} = \frac{1}{(2\pi)^{n/2}\sqrt{\det\Sigma}}\exp[-\frac{1}{2}\vec{X}^T\Sigma^{-1}\vec{X}] \tag{7}$$

The probability $P_{nh}(\vec{X})$ that no other set of $n$ hits has a lower $\chi^2$ than a fixed limit is given by the value of the Poisson distribution evaluated at 0, $\exp(-\nu_h(\vec{X}))$, where the expected number of hit sets $\nu_h(\vec{X})$ corresponds to the average number of $n$-tuplets of hits with a $\chi^2$ lower than the limit defined by $\chi^2(\vec{X})$.
In order to estimate this average number $\nu_h(\vec{X})$ we would need to know the distribution of the hits on the different measurement layers and their correlation. To simplify our computation we assume those hit distributions to be uncorrelated, uniform in 2D and equal to $\rho$[1]. The no-correlation hypothesis is not realistic because hits are generated by tracks. However it certainly represents a worst case and leads to uniform density $\rho^n$ in the $2n$-dimensional space generated by the $n$ measurements.
Because of this uniformity, the average number of hits, $\nu_h(\vec{X})$ is the density of hits in $2n$D multiplied by the $2n$-volume $E_{2n}(\vec{X})$ defining all the points $\vec{X}_p$ verifying the inequality:

$$\chi^2(\vec{X}_p) < \chi^2(\vec{X}), \tag{8}$$
$$\vec{X}_p{}^T\Sigma^{-1}\vec{X}_p < \vec{X}^T\Sigma^{-1}\vec{X}, \tag{9}$$
$$\vec{X}_p{}^T\frac{\Sigma^{-1}}{\vec{X}^T\Sigma^{-1}\vec{X}}\vec{X}_p < 1. \tag{10}$$

The latter form defines an ellipsoid in $2n$ dimensions which volume $E_{2n}(\vec{X})$ is given by:

$$E_{2n}(\vec{X}) = \frac{\pi^n}{\Gamma(1+n)}\sqrt{\det\frac{\Sigma^{-1}}{\vec{X}^T\Sigma^{-1}\vec{X}}}, \tag{11}$$
$$E_{2n}(\vec{X}) = \frac{\pi^n}{\Gamma(1+n)}(\vec{X}^T\Sigma^{-1}\vec{X})^n\sqrt{\det\Sigma}. \tag{12}$$

[1]Here, we assume that the hit density does not change from one side of the layer to the other side because the layer thickness is small enough (one or two millimeters).

So we get

$$\nu_h(\vec{X}) = \rho^n \times E_{2n}(\vec{X}), \tag{13}$$

and finally

$$\boxed{P_{nh}(\vec{X}) = \exp\Big[ -\rho^n \frac{\pi^n}{\Gamma(1+n)} (\vec{X}^T \Sigma^{-1} \vec{X})^n \sqrt{\det\Sigma}\Big].} \tag{14}$$

We can find the general expression of the matching efficiency or probability $P_{n,match}$ in the following integral form:

$$\boxed{\begin{aligned} P_{n,match} &= \frac{1}{(2\pi)^n \sqrt{\det\Sigma}} \times \int_{2nD-area} \mathrm{d}\vec{X} \\ &\exp\Big[ -\rho^n \frac{\pi^n}{\Gamma(1+n)} (\vec{X}^T \Sigma^{-1} \vec{X})^n \sqrt{\det\Sigma} - \frac{1}{2} \vec{X}^T \Sigma^{-1} \vec{X}\Big]. \end{aligned}} \tag{15}$$

## 2.3 Expression for a single-sided layer

For a single-sided layer, we have a 2 dimensional problem, $n = 1$ for which $\Gamma(1+n) = 1$, $\sqrt{\det\Sigma} = \sigma_{\mathrm{effR}\phi}\sigma_{\mathrm{effz}}$ and the search volume $V_{2n}$ is simply a rectangle of size $2f\sigma_{\mathrm{effR}\phi} \times 2f\sigma_{\mathrm{effz}}$. Thus, the formula 15 can be computed as:

$$\begin{aligned} P_{1,match} &= \int_{-f\sigma_{\mathrm{effR}\phi}}^{f\sigma_{\mathrm{effR}\phi}} \mathrm{d}x \int_{-f\sigma_{\mathrm{effz}}}^{f\sigma_{\mathrm{effz}}} \mathrm{d}z \, \frac{1}{2\pi\sigma_{\mathrm{effR}\phi}\sigma_{\mathrm{effz}}} \times \\ &\exp\Big[ -\rho\pi\sigma_{\mathrm{effR}\phi}\sigma_{\mathrm{effz}} \vec{X}^T \Sigma^{-1} \vec{X} - \frac{1}{2} \vec{X}^T \Sigma^{-1} \vec{X}\Big], \end{aligned} \tag{16}$$

$$\begin{aligned} P_{1,match} &= \int_{-f\sigma_{\mathrm{effR}\phi}}^{f\sigma_{\mathrm{effR}\phi}} \exp\Big[ -(2\rho\pi\sigma_{\mathrm{effR}\phi}\sigma_{\mathrm{effz}} + 1) \frac{x^2}{2\sigma_{R\phi}^2}\Big] \mathrm{d}x \\ &\times \int_{-f\sigma_{\mathrm{effz}}}^{f\sigma_{\mathrm{effz}}} \exp\Big[ -(2\rho\pi\sigma_{\mathrm{effR}\phi}\sigma_{\mathrm{effz}} + 1) \frac{z^2}{2\sigma_z^2}\Big] \mathrm{d}z, \end{aligned} \tag{17}$$

$$P_{1,match} = \frac{\mathrm{erf}^2(f\sqrt{\frac{1+2\pi\sigma_{\mathrm{effR}\phi}\sigma_{\mathrm{effz}}\rho}{2}})}{1 + 2\pi\sigma_{\mathrm{effR}\phi}\sigma_{\mathrm{effz}}\rho}. \tag{18}$$

These results were already obtained in [1]. If the search area is sufficiently large, $f \gg 3$, the error function can be approximated by 1 and we get the infinite search area efficiency:

$$\boxed{P_{1,match} = \frac{1}{1 + 2\pi\sigma_{\mathrm{effR}\phi}\sigma_{\mathrm{effz}}\rho}.} \tag{19}$$

This equation clearly demonstrates that, in the single-sided case, the figure of merit for the matching efficiency is the product $\sigma_{\mathrm{effR}\phi}\sigma_{\mathrm{effz}}\rho$ where each term, the two effective resolutions and the density, contribute equally to the power of 1. We also infer from equation 19 that lines with constant probability $P_{1,match}$ are hyperbolae in the planes $(\sigma_{\mathrm{effR}\phi}, \sigma_{\mathrm{effz}})$ or $(\sigma, \rho)$.

## 2.4 Expression for a double-sided layer

For a double-sided layer, we have a 4 dimensional problem, $n = 2$ for which $\Gamma(1+n) = 2$, $\sqrt{\det\Sigma} = \sigma_{\text{eff1,R}\phi}\sigma_{\text{eff1,z}} \times \sigma_{\text{eff2,R}\phi}\sigma_{\text{eff2,z}}$ and the search volume $V_{2n}$ is a 4D rectangle. Thus, the formula 15 can be computed as:

$$P_{2,match} = \frac{1}{(2\pi)^2\sigma_{\text{eff1,R}\phi}\sigma_{\text{eff1,z}}\sigma_{\text{eff2,R}\phi}\sigma_{\text{eff2,z}}} \int_{-fx_1}^{fx_1}\int_{-fz_1}^{fz_1}\int_{-fx_2}^{fx_2}\int_{-fz_2}^{fz_2} \mathrm{d}x_1\,\mathrm{d}z_1\,\mathrm{d}x_2\,\mathrm{d}z_2$$
$$\exp\Big[-\frac{\pi^2}{2}(\vec{X}^T\Sigma^{-1}\vec{X})^2\,\rho^2\,\sigma_{\text{eff1,R}\phi}\sigma_{\text{eff1,z}}\sigma_{\text{eff2,R}\phi}\sigma_{\text{eff2,z}} - \frac{1}{2}\vec{X}^T\Sigma^{-1}\vec{X}\Big]. \quad (20)$$

Contrary to the 2D case (single measurement), a second order term $(\vec{X}^T\Sigma^{-1}\vec{X})^2$ appears which prevents the easy breakdown of the 4D integral into a product of four 1D integrals. Thus, we relied on a numerical computation (Monte-Carlo integration) in this case. Similarly we observe that the density $\rho$ appears at the power of 2 in the formula.

# 3 Results

In this section, we present computation results in order to compare the two layer types: single-sided and double-sided. We remind the reader that we have assumed the hit distribution to be uncorrelated on both sides of the double-sided layer case. Our results shall then be taken as the worst matching efficiency for the latter.

As depicted in the introduction, the two sides of the double layer case are spaced only by a millimeter or two, so that we can approximate that the extrapolation of the track has the same accuracy on both sides. We also consider that the measurements on the two sides have the same uncertainty so that $\sigma_{\text{eff1,R}\phi} \approx \sigma_{\text{eff2,R}\phi} = \sigma_{\text{effR}\phi}$ and $\sigma_{\text{eff1,z}} \approx \sigma_{\text{eff2,z}} = \sigma_{\text{effz}}$. Consequently, for both cases, single-sided or double-sided, there are only three parameters on which the matching efficiency depends: the hit density $\rho$ and the two resolutions $\sigma_{\text{effR}\phi}$ and $\sigma_{\text{effz}}$. In order to represent graphically the 3D function $P_{n,match}(\rho, \sigma_{\text{effR}\phi}, \sigma_{\text{effz}})$ we will use 1D and 2D plots with respectively two or one parameters fixed and 3D surfaces of fixed probability.

For a first glimpse of the behavior of the matching efficiency we start with plotting in figure 1 the efficiency only with respect to the resolution $\sigma_{\text{effz}}$ for a fixed hit density $\rho$ and resolution $\sigma_{\text{effR}\phi}$. While the superiority of the double-sided approach is clearly observable in most of the represented conditions, a limit in hit density and effective resolution seems to appear, beyond which, the single-sided layer offers a better matching efficiency.

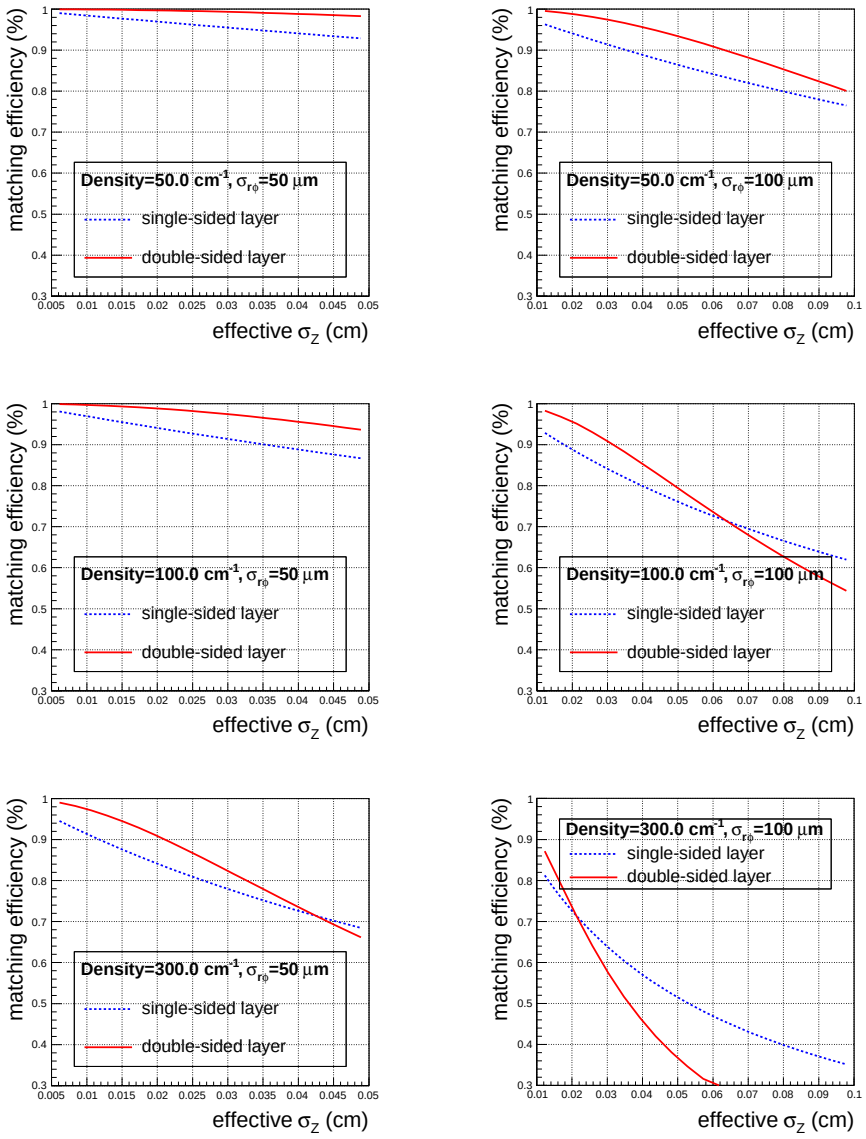


Figure 1: The matching efficiencies with respect to the effective resolution in $z$ for a hit density varying from 50 to 300 particles/cm$^2$ and an effective resolution in $R\phi$ varying from of 50 to 100 $\mu$m; in red solid for the double-sided layer case and in blue dashed line for the single-sided layer case.

To gain a better insight on this limit, the efficiency difference is computed with respect to the effective resolutions in the two directions ($R\phi$ and $z$) for two fixed hit densities 90 and 300 particles/cm$^2$, see respectively figures 2 and 3 where both resolutions are varied from 50 to 500 $\mu$m. Our choice of these ranges of parameters, is driven by the ALICE case [4]. The expected hyperbolic shape for constant matching efficiency lines is observed for the single-sided layer. The matching efficiency for the double-sided case exhibits a similar behavior but with a different curvature due to the higher order terms present in formula 20.
Thus the area for the double-sided layer, where the matching efficiency stays above[2] 90 %, extends to worst effective resolutions by 100 $\mu$m or in some places by 200 $\mu$m. Although the absolute gain in matching efficiency never exceeds about 5 % in favour of the double-sided geometry, the extension of the 90 % efficiency domain by $\mathcal{O}(100\,\mu\text{m})$ is particularly relavant for the overall tracking performance.
Beyond some limits, the single-sided layer reaches better matching efficiency (with absolute difference exceeding 15 %) but this domain corresponds to rather marginal matching efficiency values, below 60 %. On the other hand, whenever the effective resolutions are excellent, below 80 $\mu$m for 90 particles/cm$^2$ or 50 $\mu$m for 300 particles/cm$^2$, in both directions ($R\phi$ and $z$), the two geometries display no difference in efficiency.

We explore further the impact of the hit density by fixing the ratio between the two effective resolutions $\sigma_{\text{eff}z}/\sigma_{\text{eff}R\phi}$ to 1 or 3 and plotting the matching efficiency versus the hit density $\rho$ and resolution $\sigma_{\text{eff}R\phi}$ in figures 4 and 5. All our previous observations hold with these new curves.
When the conditions correspond to low hit densities combined with excellent effective resolution, the two geometries provide similar results. Performances of the two geometries depart whenever either the effective resolution or the density gets worse. The double-sided layer extents the domain where the matching efficiency stays above a given threshold. This is illustrated in the table 1 which lists the maximum densities allowed to reach significant matching efficiency thresholds with fixed effective pointing resolution conditions. We note again that the single-sided layer exhibits a better efficiency only when the absolute efficiency is quite low.

A final comparison between the two layer architectures is made through the display of the surface, in the 3D space $(\rho, \sigma_{\text{eff}R\phi}, \sigma_{\text{eff}z})$, corresponding to a fixed matching probablity, see figure 6. Any point below the surface corresponds to an efficiency above the limit. The plot clearly demonstrates how much the double-sided layer extends the satisfactory operation domain.

[2] This is of course an arbitrary threshold, nevertheless considering lower matching efficiency seems of little interest.

| Efficiency | Effective resolution ($\mu$m) | | Maximum hit density (cm$^{-2}$) | |
|---|---|---|---|---|
| | $R\phi$ | $z$ | Single | Double |
| 90% | 50 | 50 | 705 | 1265 |
| | 50 | 150 | 235 | 425 |
| 95% | 50 | 50 | 335 | 860 |
| | 50 | 150 | 110 | 285 |
| 98% | 50 | 50 | 130 | 530 |
| | 50 | 150 | 45 | 175 |
| 99% | 50 | 50 | 65 | 370 |
| | 50 | 150 | 20 | 125 |

Table 1: Comparison of maximum hit densities (provided with a $\pm 5$ cm$^{-2}$ uncertainty) to reach the 90, 95, 98 and 99 % matching efficiency levels with some fixed effective pointing resolutions in both directions for the single-sided layer and the double-sided layer.

# 4 Conclusion

In this note, we have followed an approach proposed in [1] to derive a general formula for the efficiency to match a track extrapolated to a detection layer with its corresponding hit. We have specifically explored the case of a double-sided layer which provides two equivalent measurements points separated only by one or two millimeters. We have computed the efficiency when the two measurements are considered simultaneously to better constrain the matching, under the assumption that the distribution of the hits on both layers are uncorrelated. This hypothesis certainly decreases the efficiency and hence our computation has to be considered as a worst case for the double-sided layer case. A future work based on a Monte-Carlo simulation will evaluate the impact of our assumption. Within this approach the matching is done with the hit presenting the best $\chi^2$, computed from the quadratic sum of ratios of the hit to track distance in some direction over a resolution which combines the layer spatial accuracy and the tracking extrapolation uncertainty on that layer. We found that the matching efficiency depends on an equal footing on three prominent parameters: the hit density on the layer and the two resolutions in the detection plane. From 2D graphical representations of the matching efficiency we separated the parameter space in three domains.

When all parameters are favorable, i.e. low hit density and excellent spatial accuracy, the double-sided layer and single-sided layer present equivalently good efficiency close to 100 %. When at least two parameters are disadvantageous for the matching, the efficiency for both geometries drops severly down, though the single-sided layer matches the correct hit more often. This last observa-

tion partly stems from our simplifying hypothesis that the hit distributions are independent for the two measurements of the double-sided case. In the intermediate situation where only one of the three parameters makes the matching difficult, the double-sided layer always exhibits better results for the efficiency.

The study shows that the double-sided layer allows to maintain good matching-efficiency (above 90 %), in comparison to the single-layer approach, in cases where either the hit density or the track pointing uncertainty in one of the two directions is getting large. In other cases, when both parameters are degraded, two solutions can be employed. The first one consists in decreasing the integration time of the layer to lower the hit density; it is the traditional way. Our computation clearly demonstrates that there is another way, as efficient, consisting in improving the spatial resolution of the outer layers in order to decrease the track extrapolation uncertainty on the present layer.

# References


[1] H. Wieman, V. Perevoztchikov, http://rnc.lbl.gov/~wieman/HitFinding2DXsq.htm.

[2] Z. Xu *et al.*, *A heavy flavor tracker for STAR*, LBNL-PUB-5509, Mar 7, 2006.

[3] N. Chon-Sen *et al.*, *Development of ultra-light pixelated ladders for an ILC vertex detector*, in proceedings of the 2010 International Linear Collider Workshop (LCWS10 and LC10), Beijing, 26-30 March 2010.

[4] R. Turrisi, *ALICE pixel detector operations and performance* in proceedings of *VERTEX 2010*, Proc. of Sci. (VERTEX 2010)007.

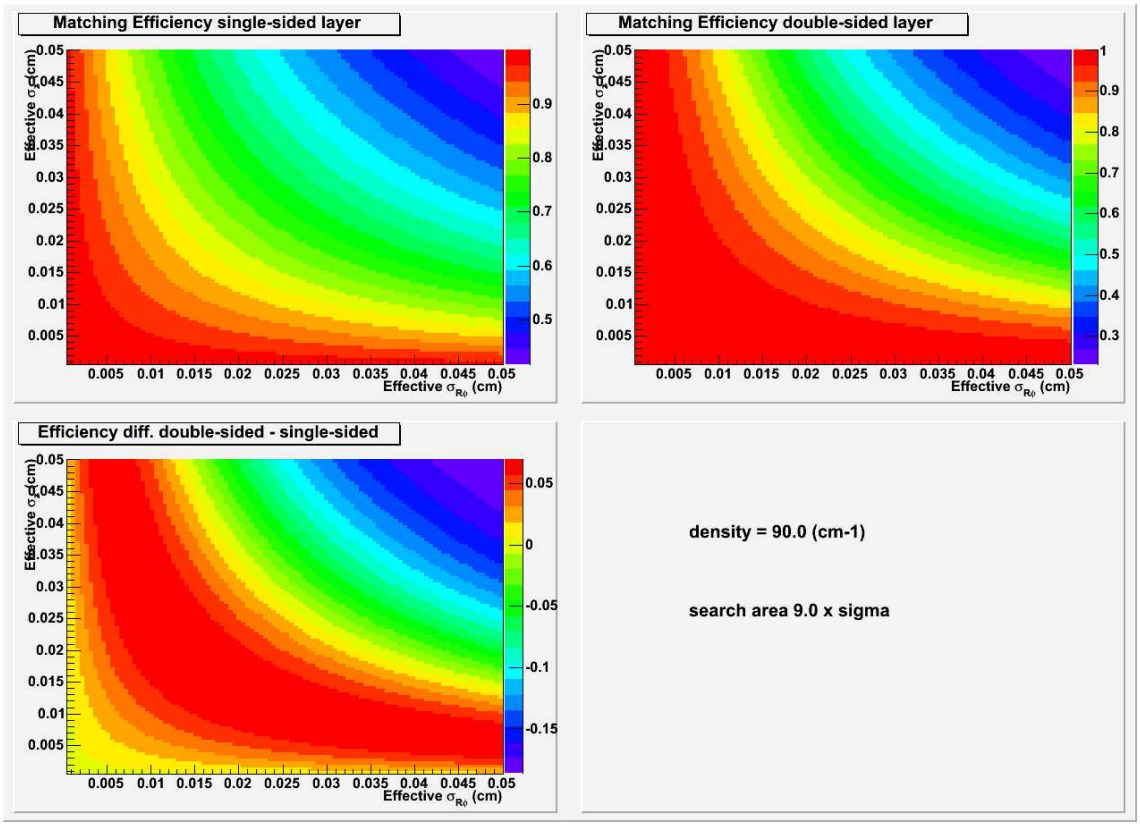


Figure 2: Top left plot shows the matching efficiency for a single-sided layer as a function of the effective resolutions in $R\phi$ and $z$ for a fixed hit density of 90 particles/cm$^2$. Top right plot shows the same quantity but for a double-sided layer. Bottom plot shows the difference between the efficiencies for the double-sided and single-sided layers.

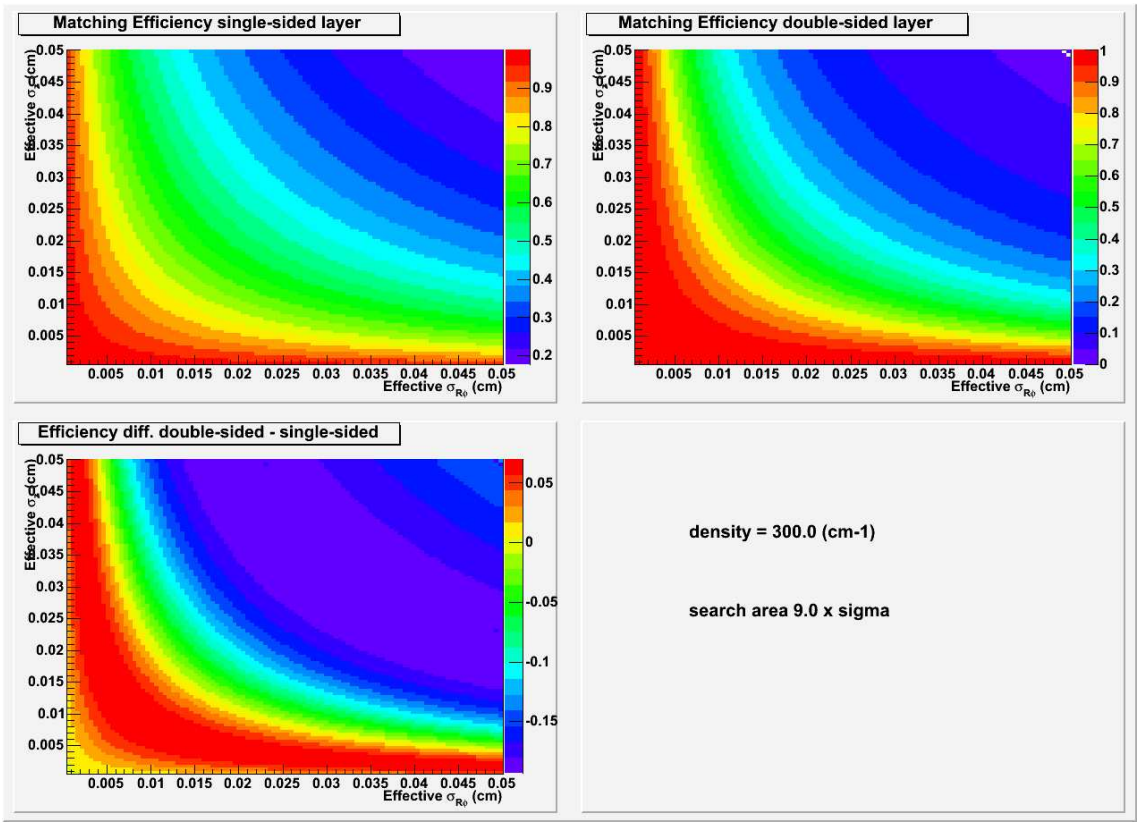


Figure 3: Top left plot shows the matching efficiency for a single-sided layer as a function of the effective resolutions in $R\phi$ and $z$ for a fixed hit density of 300 particles/cm$^2$. Top right plot shows the same quantity but for a double-sided layer. Bottom plot shows the difference between the efficiencies for the double-sided and single-sided layers.

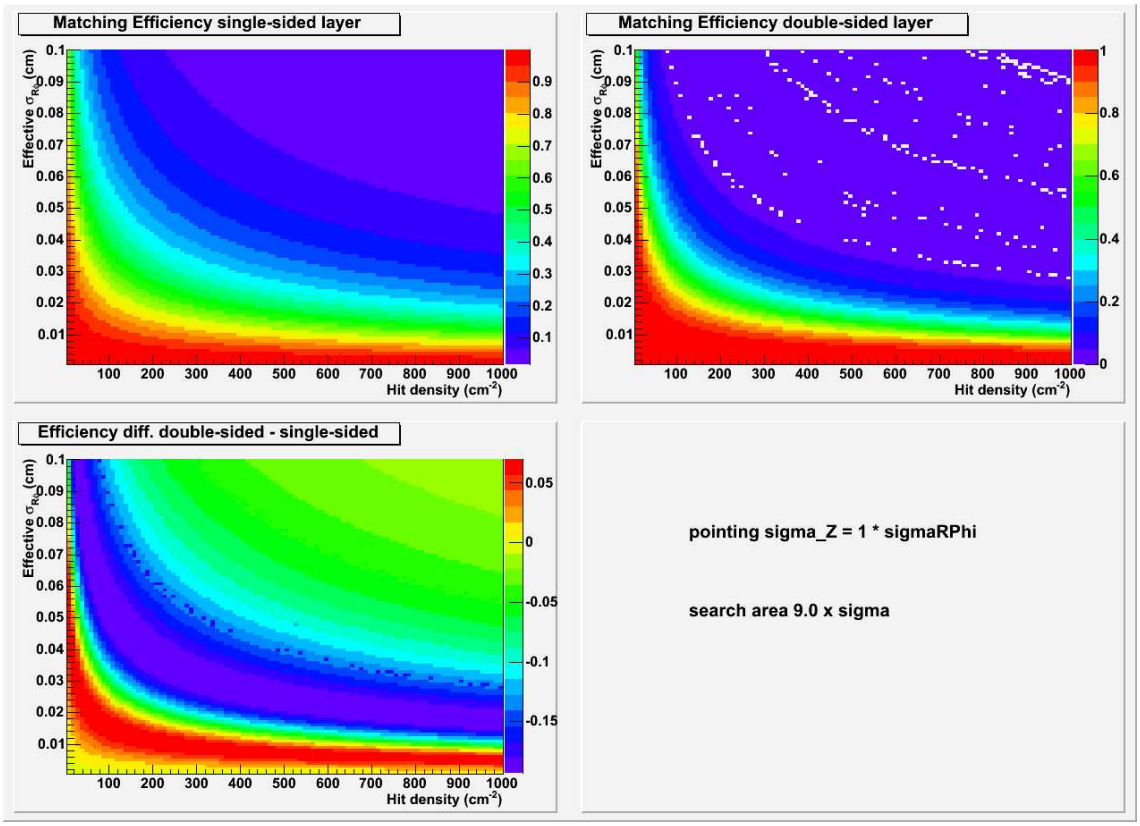


Figure 4: Top left plot shows the matching efficiency for a single-sided layer as a function of the hit density and the effective resolution in $R\phi$ for a fixed ratio $\sigma_{\mathrm{effZ}}/\sigma_{\mathrm{eff}R\phi} = 1$. Top right plot shows the same quantity but for a double-sided layer. Bottom plot shows the difference between the efficiencies for the double-sided and single-sided layers.

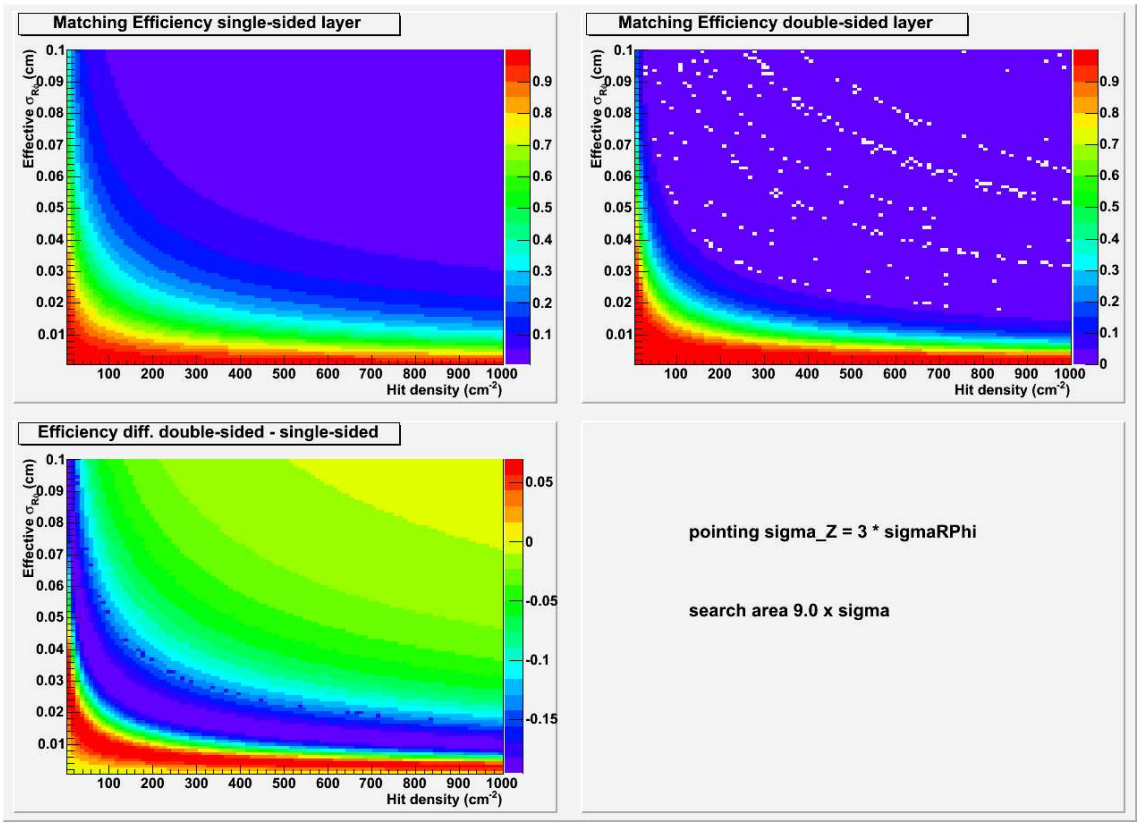


Figure 5: Top left plot shows the matching efficiency for a single-sided layer as a function of the hit density and the effective resolution in $R\phi$ for a fixed ratio $\sigma_{\mathrm{effZ}}/\sigma_{\mathrm{eff}r\phi} = 3$. Top right plot shows the same quantity but for a double-sided layer. Bottom plot shows the difference between the efficiencies for the double-sided and single-sided layers.

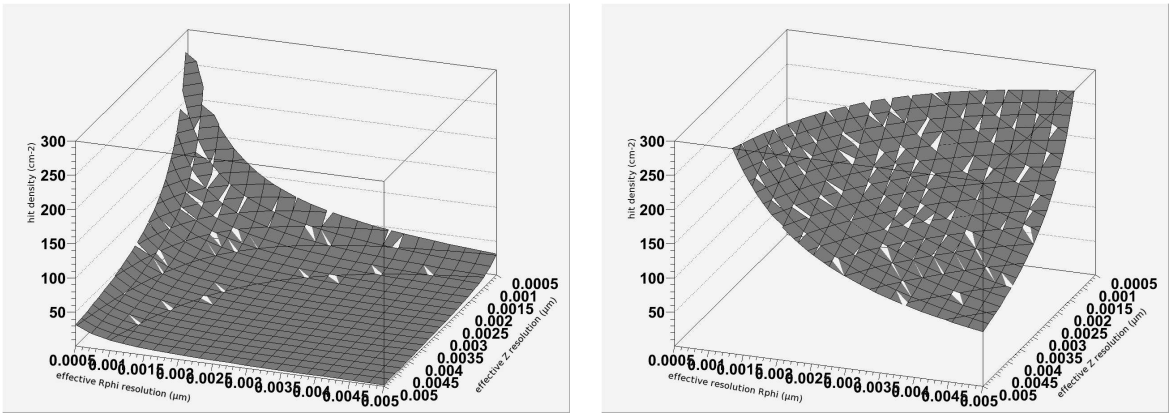


Figure 6: Surface of constant matching efficiency, here 99.95 %, for a single-sided layer on the left and for a double-sided layer on the right as a function of the effective resolutions in $R\phi$ and in $z$, and the hit density.